Volume 9, Number 6
1009-1963/2000/09(06)/0436-06
CHINESE PHYSICS
June, 2000
© 2000 Chin. Phys. Soc.

SPONTANEOUS EMISSION OF A DRIVEN FOUR-LEVEL DOPPLER BROADENED SYSTEM

YUAN SHI(袁 石) and GAO JIN-YUE(高锦岳)
Department of Physics, Jilin University, Changchun 130023, *China*

(Received 6 September 1999; revised manuscript received 22 October 1999)

We have studied the steady spontaneous emission spectrum of a four-level Doppler-broadened system driven by three coherent fields. It is found that the fluorescence spectrum is composed of nine contributions. The spectral components have quite different widths and peak heights compared with the case of the standard driven two-level or three-level resonance fluorescence. We provide numerical results in support of our arguments for arbitrary values of the atomic and field parameters.

PACC: 4250

I. INTRODUCTION

Spontaneous emission is one of the best known fundamental processes. Many theories and experiments have been reported. According to the theories,[1−4] which were confirmed by many accurate experiments,[5−8] the spectrum produced by a resonantly driven atom has sidebands which, about 1/3 as high as the central peak, are removed from the resonance by an amount proportional to the Rabi frequency of the driving field, and are wider than the central peak by a factor of 1.5. In addition, the linewidths of both the central peak and the sidebands are governed by the Einstein spontaneous decay rate in the absence of collision effects. In Ref.[9], Narducci *et al.* found that in the driven three-level system the spectral components can have different widths and peak heights compared with the standard driven two-level system.

In this paper we consider the response of a four-level atom driven by three optical fields with the aim of calculating the spontaneous emission spectrum. The system of interest is illustrated schematically in Fig.1, which includes three driving fields $\Omega_0, \Omega_1, \Omega_2$ and also an incoherent pump mechanism characterized by a pump rate R for levels $1 \rightarrow 4$. We also include the remaining spontaneous decay processes at the rates $\gamma_1, \gamma_2, \gamma_3, \gamma_4$ and γ_5.

The main result of this work is the derivation of exact formulas for the emission spectra of the $4 \rightarrow 1$ transition. Our results are valid for arbitrary strengths of the driving fields and generalize the resonance fluorescence spectra of a two-level system or a three-level system. Here we stress that the addition of a third driving field to the four-level system not only causes qualitative changes in the shape of the emission spectra, but also modifies the linewidths in a way that depends on the atomic parameters and the relative strengths of the fields.

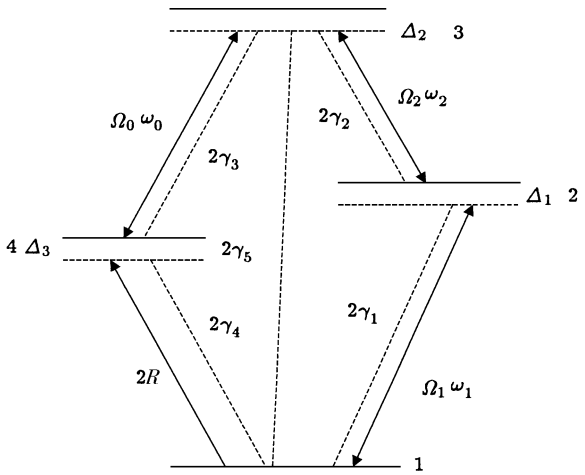


Fig.1. Schematic representation of the four-level model. $\Omega_1(\omega_1), \Omega_2(\omega_2)$ and $\Omega_3(\omega_3)$ are the Rabi frequencies (carrier frequencies) of the driving fields. The $\Delta_1, \Delta_2, \Delta_3$ and $\gamma_1, \gamma_2, \gamma_3, \gamma_4, \gamma_5$ are, respectively, detuning parameters and spontaneous decay rates. The R is the incoherent pump rate for the case $1 \rightarrow 4$.

This paper is organized as follows. In section II we derive the equations of motion and analyze the emission spectra. Section III is dedicated to a survey of the spectral results and the comparison of various predictions for different atomic configurations. In this section we also discuss the effect of Doppler broadening on the emission features of selected transitions. Here we solve the master equation for the driven atom in the limit of a strong effective Rabi frequency.

II. CALCULATION OF THE SPECTRA

Following the procedure adopted in Ref.[9], our program is carried out as follows. First, we derive the master equation for the four-level system in a semiclassical approximation, i.e., under the assumption that the three driving fields can be described by *c*-number functions. Next, We take advantage of the fact that the scattered electromagnetic field in the far zone is proportional to the atomic polarization operator for calculating the field correlation function and the spectrum of the emitted radiation. The emission spectra require knowledge of expectation values of products of operators calculated at different times; we handle these quantities with help of the quantum regression theorem.

The Hamiltonian of the four-level system interacting with three classical fields is given by

$$\begin{aligned} H =&\hbar\omega_{21}|2\rangle\langle 2| + \hbar(\omega_{32}+\omega_{21})|3\rangle\langle 3| + \hbar\omega_{41}|4\rangle\langle 4| + \hbar\Omega_1|2\rangle\langle 1|\mathrm{e}^{-\mathrm{i}\omega_1 t} + \hbar\Omega_1^*|1\rangle\langle 2|\mathrm{e}^{\mathrm{i}\omega_1 t} \\ &+ \hbar\Omega_2|3\rangle\langle 2|\mathrm{e}^{-\mathrm{i}\omega_2 t} + \hbar\Omega_2^*|2\rangle\langle 3|\mathrm{e}^{\mathrm{i}\omega_2 t} + \hbar\Omega_0|3\rangle\langle 4|\mathrm{e}^{-\mathrm{i}\omega_0 t} + \hbar\Omega_0^*|4\rangle\langle 3|\mathrm{e}^{\mathrm{i}\omega_0 t}, \end{aligned} \tag{1}$$

where $\omega_{21}, \omega_{31}, \omega_{41}$ are the atomic transition frequencies. Ω_0, Ω_1 and Ω_2 are the Rabi frequencies of the driving fields.

The interaction Hamiltonian in the interaction representation takes the from

$$\begin{aligned} H_{\mathrm{I}} =& -\hbar\Delta_1|2\rangle\langle 2| - \hbar(\Delta_1+\Delta_2)|3\rangle\langle 3| + \hbar(\Delta_3-\Delta_1+\Delta_2)|4\rangle\langle 4| + \hbar\Omega_1|2\rangle\langle 1| + \hbar\Omega_1^*|1\rangle\langle 2| \\ &+ \hbar\Omega_2|3\rangle\langle 2| + \hbar\Omega_2^*|2\rangle\langle 3| + \hbar\Omega_0|3\rangle\langle 4| + \hbar\Omega_0^*|4\rangle\langle 3|, \end{aligned} \tag{2}$$

where

$$\Delta_1 = \omega_1 - \omega_{21}, \Delta_2 = \omega_2 - \omega_{32}, \Delta_3 = \omega_0 - \omega_{34}. \tag{3}$$

The master equation for an arbitrary multi-level system is

$$\frac{\partial\rho}{\partial t} = -\frac{\mathrm{i}}{\hbar}[H_{\mathrm{I}}, \rho] + \Lambda\rho. \tag{4}$$

The relevant equation of motion for the matrix elements of the density operator (in the interaction representation) can be written in the form

$$\frac{\partial\Psi}{\partial t} = L\Psi + I, \tag{5}$$

where

$$\Psi_1 = \rho_{12},\ \Psi_2 = \rho_{13},\ \Psi_3 = \rho_{14},\ \Psi_4 = \rho_{21},\ \Psi_5 = \rho_{22},\ \Psi_6 = \rho_{23},\ \Psi_7 = \rho_{24},\ \Psi_8 = \rho_{31}, \tag{6a}$$

$$\Psi_9 = \rho_{32},\quad \Psi_{10} = \rho_{33},\quad \Psi_{11} = \rho_{34},\quad \Psi_{12} = \rho_{41},\quad \Psi_{13} = \rho_{42},\quad \Psi_{14} = \rho_{43},\quad \Psi_{15} = \rho_{44}. \tag{6b}$$

The matrix L has the explicit form

$$L_{11} = -\mathrm{i}\Delta_1 - \gamma_1 - R,\quad L_{12} = \mathrm{i}\Omega_2,\quad L_{15} = -2\mathrm{i}\Omega_1^*,\quad L_{10} = -\mathrm{i}\Omega_1^*,\quad \text{Ł}_{115} = -\mathrm{i}\Omega_1^*, \tag{7a}$$

$$L_{21} = \mathrm{i}\Omega_2^*,\quad L_{22} = -\mathrm{i}(\Delta_1+\Delta_2) - \gamma_2 - \gamma_3 - \gamma_5 - R,\quad L_{23} = \mathrm{i}\Omega_0^*,\quad L_{26} = -\mathrm{i}\Omega_1^*, \tag{7b}$$

$$L_{32} = \mathrm{i}\Omega_0,\quad L_{33} = -\mathrm{i}(\Delta_1+\Delta_2-\Delta_3) - \gamma_4 - R,\quad L_{37} = -\mathrm{i}\Omega_1^*, \tag{7c}$$

$$L_{44} = \mathrm{i}\Delta_1 - \gamma_1 - R,\quad L_{45} = 2\mathrm{i}\Omega_1,\quad L_{48} = -i\Omega_2^*,\quad L_{410} = \mathrm{i}\Omega_1,\ L_{415} = \mathrm{i}\Omega_i, \tag{7d}$$

$$L_{51} = -\mathrm{i}\Omega_1,\quad L_{54} = \mathrm{i}\Omega_1^*,\quad L_{55} = -2\gamma_1,\quad L_{56} = \mathrm{i}\Omega_2,\quad L_{59} = -\mathrm{i}\Omega_2^*,\quad L_{510} = 2\gamma_2, \tag{7e}$$

$$L_{62} = -\mathrm{i}\Omega_1,\quad L_{65} = \mathrm{i}\Omega_2^*,\quad L_{66} = -\mathrm{i}\Delta_2 - \gamma_1 - \gamma_2 - \gamma_3 - \gamma_5,\quad L_{67} = \mathrm{i}\Omega_0^*,\quad L_{610} = -\mathrm{i}\Omega_2^*, \tag{7f}$$

$$L_{73} = -\mathrm{i}\Omega_1,\quad L_{76} = \mathrm{i}\Omega_0,\quad L_{77} = -\mathrm{i}(\Delta_2-\Delta_3) - \gamma_1 - \gamma_4,\quad L_{711} = -\mathrm{i}\Omega_2^*, \tag{7g}$$

$$L_{84} = -\mathrm{i}\Omega_2,\quad L_{88} = \mathrm{i}(\Delta_1+\Delta_2) - \gamma_2 - \gamma_3 - \gamma_5 - R,\quad L_{89} = \mathrm{i}\Omega_1,\quad L_{812} = -\mathrm{i}\Omega_0, \tag{7h}$$

$$L_{95} = -\mathrm{i}\Omega_2,\quad L_{98} = \mathrm{i}\Omega_1^*,\quad L_{99} = \mathrm{i}\Delta_2 - \gamma_1 - \gamma_2 - \gamma_3 - \gamma_5,\quad L_{910} = \mathrm{i}\Omega_2^*,\quad L_{913} = -\mathrm{i}\Omega_0, \tag{7i}$$

$$L_{106} = -\mathrm{i}\Omega_2,\quad L_{109} = \mathrm{i}\Omega_2^*,\quad L_{1010} = -2\gamma_2 - 2\gamma_3 - 2\gamma_5,\quad L_{1011} = \mathrm{i}\Omega_0^*,\quad L_{1014} = -\mathrm{i}\Omega_0, \tag{7j}$$

$$L_{117} = -\mathrm{i}\Omega_2,\quad L_{1110} = \mathrm{i}\Omega_0,\quad L_{1111} = \mathrm{i}\Delta_3 - \gamma_2 - \gamma_3 - \gamma_4 - \gamma_5,\quad L_{1115} = -\mathrm{i}\Omega_0, \tag{7k}$$

$$L_{128} = -\mathrm{i}\Omega_0^*,\quad L_{1212} = \mathrm{i}(\Delta_1+\Delta_2-\Delta_3) - \gamma_4 - R,\quad L_{1213} = \mathrm{i}\Omega_1, \tag{7l}$$

$$L_{139} = -\mathrm{i}\Omega_0^*,\quad L_{1312} = \mathrm{i}\Omega_1^*,\quad L_{1313} = \mathrm{i}(\Delta_2-\Delta_3) - \gamma_1 - \gamma_4,\quad L_{1314} = \mathrm{i}\Omega_2, \tag{7m}$$

$$L_{1410} = -\mathrm{i}\Omega_0^*,\quad L_{1413} = \mathrm{i}\Omega_2^*,\quad L_{1414} = -\mathrm{i}\Delta_3 - \gamma_2 - \gamma_3 - \gamma_4 - \gamma_5,\quad L_{1415} = \mathrm{i}\Omega_0^*, \tag{7n}$$

$$L_{1510} = 2\gamma_3,\quad L_{1511} = -\mathrm{i}\Omega_0^*,\quad L_{1514} = \mathrm{i}\Omega_0,\quad L_{1415} = -2\gamma_4 + R, \tag{7o}$$

where γ_i and Δ_i are the corresponding spontaneous decay rates and detunings, respectively. R is the incoherent pump of the $1 \rightarrow 4$ transition.

The inhomogeneous vector I has nonzero components

$$I_1 = \mathrm{i}\Omega_1^*, \quad I_4 = -\mathrm{i}\Omega_1, \quad I_{15} = 2R. \tag{8}$$

The required spectrum is proportional to the Fourier transform of the two-time correlation function

$$\Gamma^{(1)}(t_1, t_0) =< P^{(-)}(t_1)P^{(+)}(t_0) >, \tag{9}$$

where $P^{(+)}(t) = \mu_{14}b_1^+ b_4, \quad P^{(-)}(t) = \mu_{41}b_4^+ b_1$.

Equation (5) must be calculated in steady state, i.e., under the double limit: $t_0, t_1 \rightarrow \infty, t_1 - t_0 = \tau > 0$, where τ is arbitrary.

Following the same procedure as described in Ref.[10], the correlation function can be cast into the required form

$$\Gamma^{(1)}(z) = \mu_{41}\mu_{14}\left\{\{M_{31}(z)\,\Psi_{13}(\infty) + M_{32}(z)\,\Psi_{14}(\infty) + M_{33}(z)\,\Psi_{15}(\infty)\} + \frac{1}{z}\sum_{j=1}^{15} M_{3j}(z)I_j\,\Psi_{12}(\infty)\right\}, \tag{10}$$

where $\Psi_i(\infty) = -\sum_{j=1}^{15}(L^{-1})_{ij}I_j$ denotes the ith stationary matrix element of the density operator.

After elimination of the coherent part, the spectrum of the radiated fluorescence is given by

$$S(\omega) = \mathrm{Re}\hat{\Gamma}^{(1)}_{\mathrm{incoh}}(z)|_{z=\mathrm{i}(\omega-\omega_1-\omega_2+\omega_0)}, \tag{11}$$

where $\hat{\Gamma}^{(1)}_{\mathrm{incoh}}(z)$, the so-called incoherent part of the Laplace transform of $\Gamma^{(1)}(z)$, has the explicit form

$$\hat{\Gamma}^{(1)}_{\mathrm{incoh}}(z) = M_{31}(z)\,\Psi_{13}(\infty) + M_{32}(z)\,\Psi_{14}(\infty) + M_{33}(z)\,\Psi_{15}(\infty) + \sum_{j=1}^{15} N_{3j}(z)I_j\,\Psi_{12}(\infty), \tag{12a}$$

$$M_{ij}(z) = [(z-L)^{-1}]_{ij}, \tag{12b}$$

$$N_{ij}(z) = [L^{-1}(z-L)^{-1}]_{ij}. \tag{12c}$$

Ⅲ. A SURVEY OF THE NUMERICAL RESULTS

This section contains a graphical survey of some specific predictions that emerge from the formulas derived in Sec. II. In the calculations, we scale all the detunings and field Rabi frequencies in terms of γ_4. We find there can be striking differences between the fluorescence produced by an atom driven by two(one) or three resonant fields. First, we consider the situation that only one driving field is turned on. For this case, we plot the fluorescence spectrum in Fig.2.

Figures 2(a) and 2(b) illustrate the typical incoherent part of the spectrum in Ref.[11] produced by the $4 \rightarrow 1$ spontaneous decay of the four-level system when only one driving field is turned on. In Ref.[11], Zhu *et al.* named Figs.2(a) and 2(b) the lower level coupling, and upper level coupling respectively. As we expected, Fig.2(c) is composed of a single peak. Secondly, we see the situation that there are only two driving fields turned on. The spectrum is shown in Fig. 3.

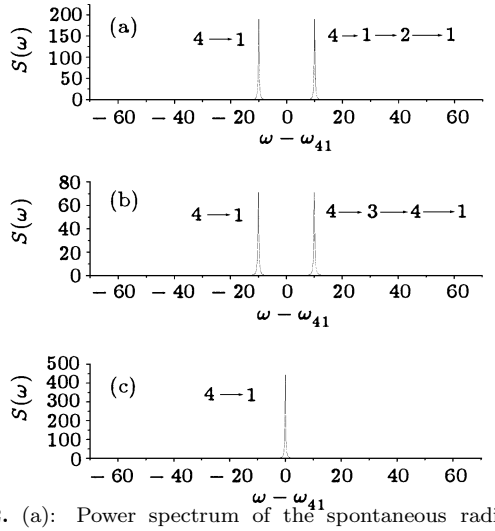


Fig.2. (a): Power spectrum of the spontaneous radiation emitted by the 4→1 transition for $\Omega_1 = 10, \Omega_0 = 0, \Omega_2 = 0, R = 0.1, \Delta_1 = \Delta_2 = \Delta_3 = 0, \gamma_1 = \gamma_2 = \gamma_3 = \gamma_5 = 0.05$; (b): same as curve (a), except that $\Omega_1 = 0, \Omega_0 = 10, \Omega_2 = 0$; (c): same as curve (a), except that $\Omega_1 = 0, \Omega_0 = 0, \Omega_2 = 10$.

Figures 3(a) and 3(b) illustrate the typical appearance of three spectral components in resonance; one centers at the atomic transition frequency and two symmetric pairs of sidebands separated by $\pm\Omega$ from the center, where $\Omega = (\Omega_1^2 + \Omega_2^2)^{1/2}$ in Fig.3(a) and $\Omega = (\Omega_0^2 + \Omega_2^2)^{1/2}$ in Fig.3(b). The central peak and the sidebands have a Lorentzian profile whose widths and peak heights agree with those quoted in Refs.[9,

10]. In Fig.4 we plot the curve with $\Omega_1 \neq 0, \Omega_0 \neq 0, \Omega_2 = 0$.

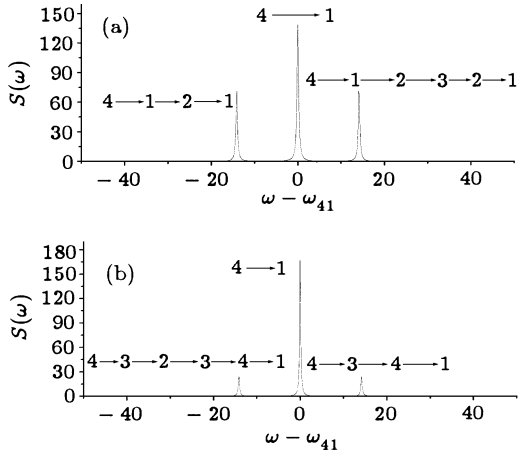


Fig.3. (a): Power spectrum of the spontaneous radiation emitted by the $4 \rightarrow 1$ transition for $\Omega_1 = 10, \Omega_0 = 0, \Omega_2 = 10$; (b): same as curve (a), except that $\Omega_1 = 0, \Omega_0 = 10, \Omega_2 = 10$, other parameters are same as Fig.2.

Figure 4(a) shows three spectral components in resonance. The reason is that $\Omega_1 = \Omega_0$, so the original four spectral components evolve into three spectral components. We can see this point from Figs. 4(b) and 4(c) with $\Omega_1 \neq \Omega_0$. In Fig.4(b), the frequency spacing between component 1 and component 2(3) and 4) is Ω_1, and the frequency spacing from the middle of the lines 1 and 2 to the middle of the lines 3 and 4 is Ω_0. The analysis of Fig.4(c) is same as Fig.4(b).

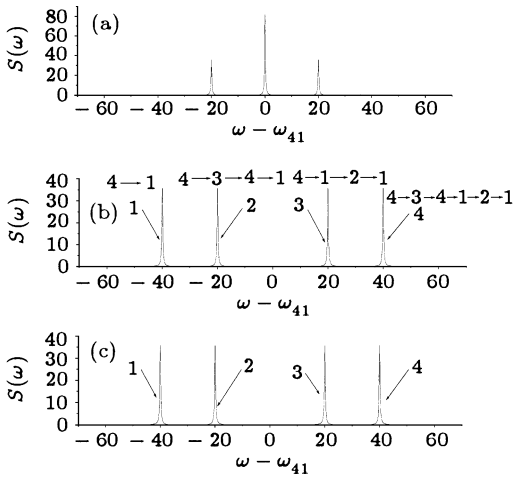


Fig.4. (a): Power spectrum of the spontaneous radiation emitted by the $4 \rightarrow 1$ transition for $\Omega_1 = 10, \Omega_0 = 10, \Omega_2 = 0$; (b): same as curve (a), except that $\Omega_1 = 10, \Omega_0 = 7, \Omega_2 = 0$; (c): same as curve (a), except that $\Omega_1 = 7, \Omega_0 = 10, \Omega_2 = 0$, other parameters are same as Fig.2.

All of the above results can be explained in the dressed atomic state representation. Since there are many papers[9,10] which gave the explanation about the fluorescence spectrum with two driving fields, here we do not give the results again. But we will give another explanation about the above results by using the decay pathways from level 4 to level 1. We give some examples. When only driving field Ω_1 is turned on, we see two decay pathways $4 \rightarrow 1$ and $4 \rightarrow 1 \rightarrow 2 \rightarrow 1$. The two pathways lead to two distinct components, as confirmed by the explicit calculations in Fig.2(a). And when only two driving fields Ω_1 and Ω_0 are turned on, there are four decay pathways (1) $4 \rightarrow 1$; (2) $4 \rightarrow 3 \rightarrow 4 \rightarrow 1$; (3) $4 \rightarrow 3 \rightarrow 4 \rightarrow 1 \rightarrow 2 \rightarrow 1$ and (4) $4 \rightarrow 1 \rightarrow 2 \rightarrow 1$.This results in four spectral structures in Fig.4(b). Although we can only give the final numerical results, all of the above confirm that our results are correct.

However, so far, the published papers about fluorescence spectrum are limited to the systems driven by two driving fields. Here we consider the case having three driving fields ($\Omega_0 \neq 0, \Omega_1 \neq 0, \Omega_2 \neq 0$). We find that there are many differences between the fluorescence produced by an atom driven by two and by three resonant fields. Figure 5 illustrates the role of the spectrum in resonance with $\Omega_1 = 10, \Omega_0 = 12, \Omega_2 = 7$.

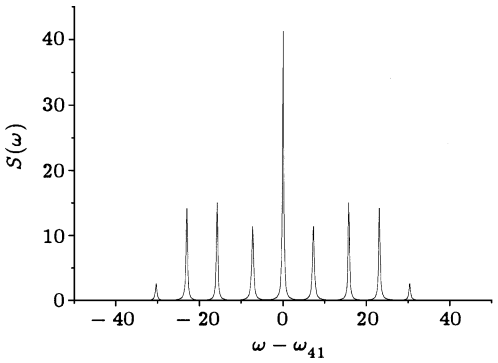


Fig.5. Power spectrum of the spontaneous radiation emitted by the $4 \rightarrow 1$ transition for $\Omega_1 = 10, \Omega_2 = 7, \Omega_0 = 12$.

Now we give an explanation by using the decay pathways from level 4 to level 1. From Fig.1, we could expect that the spectrum might consist of nine main components, which are represented by nine decay pathways: (1) $4 \rightarrow 1$; (2) $4 \rightarrow 3 \rightarrow 4 \rightarrow 1$; (3) $4 \rightarrow 3 \rightarrow 2 \rightarrow 3 \rightarrow 4 \rightarrow 1$; (4) $4 \rightarrow 3 \rightarrow 2 \rightarrow 1$; (5) $4 \rightarrow 3 \rightarrow 2 \rightarrow 1 \rightarrow 2 \rightarrow 3 \rightarrow 4 \rightarrow 1$; (6)$4 \rightarrow 1 \rightarrow 2 \rightarrow 1$; (7) $4 \rightarrow 1 \rightarrow 2 \rightarrow 3 \rightarrow 2 \rightarrow 1$; (8) $4 \rightarrow 1 \rightarrow 2 \rightarrow 3 \rightarrow 4 \rightarrow 1$; (9) $4 \rightarrow 1 \rightarrow 2 \rightarrow 3 \rightarrow 4 \rightarrow 3 \rightarrow 2 \rightarrow 1$.

A clear picture of the dependence of the peak heights and linewidths on the Rabi frequency of the third field Ω_2 is shown in Figs.6 and 7. We can see

that the dependence of the widths and peak heights of the nine components on Ω_2 are different from one another.

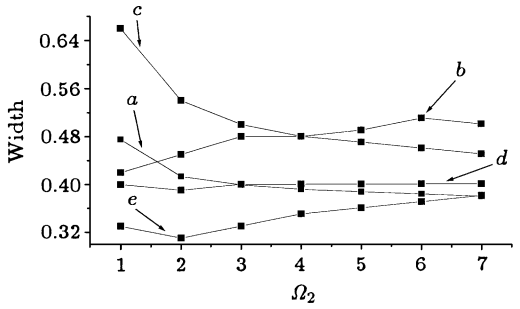


Fig.6. Dependence of the linewidths of the spectral components of the $4 \rightarrow 1$ spectrum upon the Rabi frequency Ω_2. Curves $a-e$ represent the widths of the central component and sidebands.

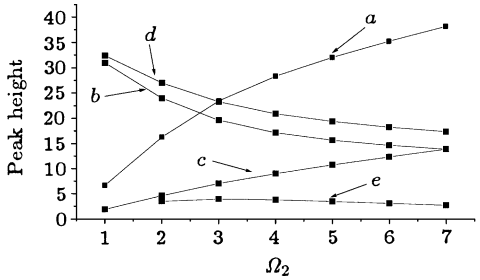


Fig.7. Dependence of the peak heights of the spectral components of the $4 \rightarrow 1$ spectrum upon the Rabi frequency Ω_2. Curves $a-e$ represent the peaks of the central component and sidebands.

Finally, we consider the effects of the Doppler broadening on the spectrum. The frequencies of the three fields in the atomic frame should be velocity dependent

$$\omega_1' = \omega_1(1 - V_y/C), \quad \omega_2' = \omega_2(1 - V_y/C), \omega_0' = \omega_0(1 - \eta V_y/C) \quad (\eta = \pm 1), \tag{13}$$

where V_y is the atomic velocity component along the propagating direction of the field ω_1; $\eta = 1$ refers to the case when ω_0 and ω_1 are co-propagating, while $\eta = -1$ refers to the case when ω_0 and ω_1 are counter-propagating. In the calculation we keep that ω_1 and ω_2 are co-propagating. If we replace $\omega_1, \omega_2, \omega_0$ with $\omega_1', \omega_2', \omega_0'$ in the calculation of the fluorescence spectrum in Eq.(11), we get a fluorescence spectrum of the atoms in the atomic coordinates

$$< \hat{\Gamma}^{(1)}_{\rm incoh}(z) >= \int_{\Delta_1 - 4\omega_{\rm D}}^{\Delta_1 + 4\omega_{\rm D}} P(\delta_1)(\hat{\Gamma}^{(1)}_{\rm incoh}(z))\mathrm{d}\delta_1, \tag{14}$$

where

$$\delta_1 = \Delta_1 + \omega_1 V_y/C, \tag{15}$$

$$Z = \mathrm{i}(\omega - (\omega_{21} + \omega_{32} - \omega_{34}) + (\Delta_1 + \Delta_2 - \Delta_3) + (\delta_1 - \Delta_1) + (1 + \omega_2/\omega_1) - \eta(\delta_1 - \Delta_1)\omega_0/\omega_1), \tag{16}$$

$$P(\delta_1) = \left[\frac{\pi\omega_{\rm D}^2}{4\ln 2}\right]^{-1/2} \exp\left[\frac{-4\ln 2(\delta_1 - \Delta_1)^2}{\omega_{\rm D}^2}\right], \tag{17}$$

$$\omega_{\rm D} = \frac{\omega_1}{C}\left[\frac{8KT\ln 2}{M}\right]^{1/2}, \tag{18}$$

where $\omega_{\rm D}$ is Doppler broadening.Figure. 8 shows the calculated results.

Figure 8(a) with $\omega_{\rm D} = 1.0$ corresponds to the very small Doppler broadening case, while Figs. 8(b) and 8(c) with $\omega_{\rm D} = 10.0$ correspond to the Doppler broadening cases when ω_0 and ω_1 are co- and counter-propagating, respectively. From Figs. 8(b) and 8(c), we can conclude that when ω_0 and ω_1 are counter-propagating, the resolution of the three-driving-field

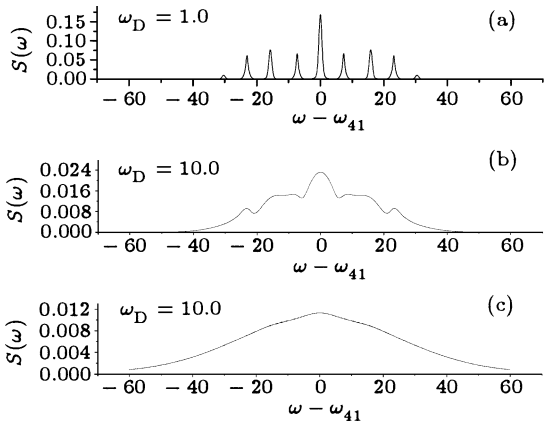


Fig.8. Power spectrum of the spontaneous radiation emitted by the $4 \rightarrow 1$ transition for $\Omega_1 = 10, \Omega_2 = 7, \Omega_0 = 12$; (a) is the small Doppler broadening, $\omega_{\rm D} = 1.0$; (b) and (c),$\omega_{\rm D} = 10.0$, corresponding to the Doppler broadening cases when ω_0 and ω_1 are co- and counter-propagating, respectively.

fluorescence profiles is more or less independent of Doppler broadening, but in the case when ω_0 and ω_1

are co-propagating, the Doppler broadening mekes the fluorescence minimum increase and the resolution of the fluorescence profiles decrease.

In summary, we have studied the steady spontaneous emission spectrum of a four-level Doppler-broadened system driven by three coherent fields, and given a numerical calculation results. We find that the fluorescence spectrum is composed of nine contributions and the spectral components have quite different widths and peak heights compared with the case of the standard driven two-level or three-level resonance fluorescence. We also provide the best arrangement of these three laser-propagating directions for reducing the Doppler effects in this system.

REFERENCES

[1] M.C.Newstein, *Phys. Rev.,* **167**(1968), 89.

[2] B.R.Mollow, *Phys. Rev.,***188**(1969), 1969; *Phys. Rev.,* **A2** (1970), 76.

[3] C.R.Stroud, Jr., *Phys. Rev.,* **A3**(1971), 1044.

[4] G.S. Agarwal, *Phys. Rev.,* **A2**(1970), 2038;**4**(1971), 1778.

[5] W. Hartig, H. Walther,*Appl. Phys.,***1**(1973), 171.

[6] F.Shuda, C.R.Stroud, Jr., M. Hercher, *J. Phys.,* **B7**(1974), L198.

[7] F.Y.Wu, R.E.Grove, S.Ezekiel, *Phys.Rev.Lett.,***35**(1975), 1426.

[8] H.Walther, in Conference, Megeve, France, Proceedings of the Second Spectroscopy (1974), edited by S. Haroche, J. C. Pebay-Peyroula, T.W. Hansch *et al.* (Springer-Verlag, Berlin, 1975), p.358.

[9] L.M.Narducci,M.O.Scully, G.L.Oppo *et al., Phys. Rev.,* **A42**(1990), 1630.

[10] A.S.Manka, H.M. Doss, L.M. Narducci *et al., Phys. Rev.,* **A43**(1991), 3748.

[11] S. Y. Zhu, L. M. Narducci, M. O. Scully, *Phys., Rev.,***A52**(1995), 4791.